IEICE TRANS. FUNDAMENTALS, VOL.E82–A, NO.4 APRIL 1999

PAPER *Special Section on Advanced Signal Processing Techniques for Analysis of Acoustical and Vibrational Signals*

PARCORR-Based Time-Dependent AR Spectrum Estimation of Heart Wall Vibrations

Hiroshi KANAI[†], ***Member and*** **Yoshiro KOIWA**[††], ***Nonmember***

SUMMARY We present a new method for estimation of spectrum transition of nonstationary signals in cases of low signal-to-noise ratio (SNR). Instead of the basic functions employed in the previously proposed time-varying autoregressive (AR) modeling, we introduce a spectrum transition constraint into the cost function described by the partial correlation (PARCORR) coefficients so that the method is applicable to noisy nonstationary signals of which spectrum transition patterns are complex. By applying this method to the analysis of vibration signals on the interventricular septum (IVS) of the heart, noninvasively measured by the novel method developed in our laboratory using ultrasonics, the spectrum transition pattern is clearly obtained during one cardiac cycle for normal subjects and a patient with cardiomyopathy.

key words: *time-dependent spectrum estimation, AR modeling, noninvasive diagnosis*

1. Introduction

Much work has been done on parametric spectrum estimation using the autoregressive (AR) model. A strong restriction of methods based on this model lies in the necessary assumption that the signals may be considered to be stationary during the observation period. Time-varying parametric approaches of modeling have been proposed to overcome this limitation and to take the effects of nonstationary signals into account explicitly. To estimate the parameters using a linear algorithm, the unknown time-varying parameters are approximated by linearly weighted combinations of a small number of known functions. The choice of the basic functions is an important part of such a modeling process. A convenient way is to replace the time-varying coefficients with their second-order expansion [1] or an arbitrary order expansion [2], [3]. Legendre [4], [5], Fourier [6], prolate spheroidal [7], and B-spline [8] are the basic functions usually chosen. Since the number of unknown parameters is large, efficient equivalent representations for the modeling, such as lattice filters, have also been proposed [2], [7], [9].

However, if the spectrum transition pattern is complex and/or there are large differences in the transition patterns among the individual nonstationary signals, it is difficult to estimate the transition pattern stably by choosing a set of basic functions *a priori*.

We have proposed a method for analyzing the spectrum transition of the multi-frame signals of the fourth heart sounds detected during the stress test [10]. In this method, however, the signals which can be analyzed are limited to *multiple short length signals*; the spectrum transition patterns between these signals are obtained. In this paper, by modifying this method, we propose a new approach of modeling to estimate the spectrum transition of *a nonstationary signal* by using a *linear algorithm* without any basic functions.

In this paper, moreover, we describe the spectrum transition constraint not by the linear predictive coefficients of the AR model but by the *partial correlation* (*PARCORR*) *coefficients*. In the method developed in [10], the cost function of the multi-frame signals is defined by the sum of the residual powers in the AR modeling and the spectrum transition between the multi-frame signals. The latter component of the spectrum transition is defined by the sum of the differences of the linear predictive coefficients $\{a_i\}$ between the successive frames. In general, however, the values of the coefficients $\{a_i\}$ are large at low order and small at high order. Thus, it is significant to determine the weight of each order of the coefficients $\{a_i\}$ in the summation process.

For this problem, in this paper, the PARCORR coefficients $\{k_i\}$ instead of the linear predictive coefficients $\{a_i\}$ are introduced into the definition of the cost function. Since the range of the PARCORR coefficients $\{k_i\}$ is from -1 to $+1$ even in low and high orders, it is not necessary to consider the weights in the definition of the spectrum transition of the cost function.

To noninvasively diagnose the acoustic characteristics of the heart muscle, it is necessary to measure the small vibration signals on the heart wall from the chest surface with enough accuracy to permit analysis in the frequency range up to at least 100 Hz and analysis of the resultant nonstationary signal continuously during one cardiac cycle.

For the problem of the noninvasive measurement described above, we have already developed a novel method for accurate ultrasonic-based measurement of small velocity signals on and in the heart wall in the frequency range up to several hundred Hertz [11]–[13].

Manuscript received August 17, 1998.
Manuscript revised November 11, 1998.

[†]The author is with the Department of Electrical Engineering, Graduate School of Engineering, Tohoku University, Sendai-shi, 980–8579 Japan.
[††]The author is with the First Department of Internal Medicine, School of Medicine, Tohoku University, Sendai-shi, 980–8578 Japan.

If non-stationary spectrum analysis is applied to the resultant velocity signals, more detailed information on the heart function can be obtained. To solve the problem of the spectrum analysis, we apply the novel time-varying modeling developed in this paper to the nonstationary small vibration signals on the interventricular septum (IVS) to diagnose the acoustic characteristics of the heart muscle. These characteristics and the transition patterns show the potential of the proposed method for the noninvasive diagnosis of heart diseases.

2. Principle of Spectrum Estimation Using PARCORR Coefficients

Let us divide an original nonstationary signal $x(n)$ into successive F short signals $\{x_j(n)\}$, $n = 0, 1, \ldots, N-1$, $j = 0, 1, \ldots, F-1$, each called a *frame*, where F is the number of frames. Let us assume that each frame signal $x_j(n)$ is an AR signal of order M, represented by the forward and backward recursions. The order M of the AR model coincides with double the number of the poles in the frequency range up to the Nyquist frequency. The number of poles is physically determined by the eigen-vibration systems. During the whole analyzed period of the original nonstationary signal $x(n)$, let us assume that the eigen-vibration systems do not vary and that only their eigen-frequencies vary. In this paper, therefore, we assume that the all of the frame signals are of the same order M.

The forward predictive error $e^f_{M,j}(n)$ and the backward predictive error $e^b_{M,j}(n)$ of M-order prediction are respectively given by

$$e^f_{M,j}(n) = \sum_{i=0}^{M} a_{Mi,j} \cdot x_j(n-i), \tag{1}$$

$$e^b_{M,j}(n-M-1) = \sum_{i=0}^{M} b_{Mi,j} \cdot x_j(n-i-1), \tag{2}$$

where $\{a_{Mi,j}\}$ and $\{b_{Mi,j}\}$ are ith order forward and backward predictive coefficients, respectively, of jth frame data, $a_{M0,j} = 1$ and $b_{MM,j} = 1$. When the predictive order is equal to M, the average power $\alpha_{M,j}$ of the predictive error for the data in the period $[M, N-1]$ of jth frame data is given by

$$\begin{aligned}\alpha_{M,j} &= \frac{1}{N-M}\sum_{n=M}^{N-1} |e^f_{M,j}(n)|^2 \\ &= \sum_{i=0}^{M}\sum_{\ell=0}^{M} a_{Mi,j} a_{M\ell,j} C_{i\ell,j},\end{aligned} \tag{3}$$

where $C_{i\ell,j}$ is the covariance matrix of data $x_j(n)$ defined by

$$C_{i\ell,j} = \frac{1}{N-M}\sum_{n=M}^{N-1} x_j(n-i)\cdot x_j(n-\ell). \tag{4}$$

By minimizing $\alpha_{M,j}$ with respect to the forward predictive coefficients $\{a_{Mi,j}\}$, the resultant normal equation is given by

$$\frac{1}{2}\frac{\partial \alpha_{M,j}}{\partial a_{Mi,j}} = \sum_{\ell=0}^{M} a_{M\ell,j}\cdot C_{i\ell,j} = 0 \quad (i = 1, 2, \ldots, M) \tag{5}$$

Equation (5) is rewritten as follows:

$$\sum_{\ell=1}^{M} C_{i\ell,j}\cdot a_{M\ell,j} = -C_{i0,j}. \quad (i = 1, 2, \ldots, M) \tag{6}$$

For the backward prediction, on the other hand, it is well-known [14], [15] that the backward predictive error signal $e^b_{M-1,j}(n-M)$ in the $(M-1)$th order prediction should be orthogonal to the $(M-1)$th order backward predictor, $\widehat{x}^b_{M-1,j}(n-M) = \sum_{i=0}^{M-2} b_{M-1,i,j} x_j(n-1-i)$, of the jth frame signal, that is,

$$\frac{1}{N-M}\sum_{n=M}^{N-1}\left[e^b_{M-1,j}(n-M) \times \left(\sum_{i=0}^{M-2} b_{M-1,i,j} x_j(n-1-i)\right)\right] = 0. \tag{7}$$

From this equation, for the cases of $p > q$, the error series $e^b_{p-1,j}(n-p)$ is orthogonal to each of the components $x_j(n-p+1), x_j(n-p+2), \ldots, x_j(n-1)$ of the backward predictor $\widehat{x}^b_{p-1,j}(n-p)$. Thus,

$$\frac{1}{N-M}\sum_{n=M}^{N-1} e^b_{p-1,j}(n-p)\cdot e^b_{q-1,j}(n-q) = 0. \quad (p > q) \tag{8}$$

For the case of $p = q$, however, by defining a nonnegative constant $\delta_{p,j}$, the following relation is obtained:

$$\begin{aligned}\delta_{p,j} &= \frac{1}{N-M}\sum_{n=M}^{N-1}\left|e^b_{p-1,j}(n-p)\right|^2 \\ &= \sum_{i=0}^{p-1}\sum_{\ell=0}^{p-1} b_{p-1,i,j} b_{p-1,\ell,j} C_{i+1,\ell+1,j}.\end{aligned} \tag{9}$$

Moreover, it is well-known [14], [15] that the forward predictive coefficient $a_{Mi,j}$ is recursively derived from the results estimated up to the $(M-1)$th order as follows:

$$a_{Mi,j} = a_{M-1,i,j} + k_{M,j} b_{M-1,i-1,j}, \quad (i = 1, 2, \ldots, M-1) \tag{10}$$

where the term $k_{M,j}$ is the PARCORR coefficient for jth frame data. From this recursion,

$$a_{Mi,j} = (a_{M-2,i,j} + k_{M-1,j} b_{M-2,i-1,,j})$$

$$
\begin{aligned}
&+ k_{M,j} b_{M-1,i-1,j} \\
&= \cdots \\
&= (a_{1i,j} + k_{2,j} b_{1,i-1,,j}) + k_{3,j} b_{2,i-1,,j} + \cdots \\
&\quad + k_{M,j} b_{M-1,i-1,,j} \\
&= k_{1,j} + \sum_{\ell=2}^{M} k_{\ell,j} b_{\ell-1,i-1,j}, \qquad (11)
\end{aligned}
$$

where the relation $a_{1i,j} = k_{1,j}$ is employed.

Let us respectively define M-dimension vectors $\mathbf{a}_j$, $\mathbf{k}_j$, $\mathbf{c}_j$, an $(N-M)$-dimension vector $\mathbf{x}_j$, an $M \times M$ upper triangle matrix $\mathbf{B}_j$, an $M \times M$ diagonal matrix $\mathbf{\Delta}_j$, and an $M \times M$ covariance matrix $\mathbf{C}_j$, which is positive definite, by

$$\mathbf{a}_j = [a_{M1,j}, a_{M2,j}, \cdots, a_{MM,j}]^T, \qquad (12)$$

$$\mathbf{k}_j = [k_{M1,j}, k_{M2,j}, \cdots, k_{MM,j}]^T, \qquad (13)$$

$$\mathbf{c}_j = [C_{10,j}, C_{20,j}, \cdots, C_{M0,j}]^T, \qquad (14)$$

$$\mathbf{x}_j = \frac{1}{\sqrt{N-M}} [x_j(M), \cdots, x_j(N-1)]^T, \qquad (15)$$

$$\mathbf{B}_j = \begin{bmatrix} 1 & b_{10,j} & b_{20,j} & \cdots & b_{M-1,0,j} \\ 0 & 1 & b_{21,j} & \cdots & b_{M-1,1,j} \\ 0 & 0 & 1 & \ddots & \vdots \\ \vdots & \ddots & \ddots & \ddots & b_{M-1,M-2,j} \\ 0 & \cdots & \cdots & 0 & 1 \end{bmatrix}, \qquad (16)$$

$$\mathbf{\Delta}_j = \begin{bmatrix} \delta_{1j} & 0 & \cdots & 0 \\ 0 & \delta_{2j} & \cdots & 0 \\ \vdots & 0 & \ddots & \vdots \\ 0 & \cdots & 0 & \delta_{M,j} \end{bmatrix}, \qquad (17)$$

$$\mathbf{C}_j = [C_{i\ell,j}]. \qquad (18)$$

Using these vectors and matrices, Eqs. (6), (11), and (8), Eq. (9) are respectively simplified as

$$\mathbf{C}_j \cdot \mathbf{a}_j = -\mathbf{c}_j, \qquad (19)$$

$$\mathbf{a}_j = \mathbf{B}_j \cdot \mathbf{k}_j, \qquad (20)$$

$$\mathbf{B}_j^T \cdot \mathbf{C}_j \cdot \mathbf{B}_j = \mathbf{\Delta}_j. \qquad (21)$$

Thus, the total power $\alpha_{M,j}$ of the Mth-order forward predictive error in Eq. (3) is given by using the PARCORR coefficients as follows:

$$
\begin{aligned}
\alpha_{M,j} &= \mathbf{a}_j^T \mathbf{C}_j \mathbf{a}_j + 2\mathbf{c}_j^T \mathbf{a}_j + \mathbf{x}_j^T \mathbf{x}_j \\
&= \mathbf{k}_j^T \mathbf{B}_j^T \mathbf{C}_j \mathbf{B}_j \mathbf{k}_j + 2\mathbf{c}_j^T \mathbf{B}_j \mathbf{k}_j + \mathbf{x}_j^T \mathbf{x}_j \\
&= \mathbf{k}_j^T \mathbf{\Delta}_j \mathbf{k}_j + 2(\mathbf{B}_j^T \mathbf{c}_j)^T \mathbf{k}_j + \mathbf{x}_j^T \mathbf{x}_j. \qquad (22)
\end{aligned}
$$

3. Principle of Estimation of Spectrum Transition

When each frame of the multi-frame nonstationary signal $\{\mathbf{x}_j\}$ $(j = 0, 1, \ldots, F-1)$ is described by the AR model, based on Eq. (22), let us define the logarithmic likelihood function ℓ, which shows the probability of $\{\mathbf{x}_j\}$ for unknown PARCORR coefficients $\{\mathbf{k}_j\}$, by

$$
\begin{aligned}
\ell = -\sum_{j=0}^{F-1} \Bigg\{ & \frac{\mathbf{k}_j^T \mathbf{\Delta}_j \mathbf{k}_j + 2(\mathbf{B}_j^T \mathbf{c}_j)^T \mathbf{k}_j + \mathbf{x}_j^T \mathbf{x}_j}{|\mathbf{x}_j|^2} \\
& + \lambda_j \left| \mathbf{k}_{j+1} - \mathbf{k}_j \right|^2 \Bigg\}, \qquad (23)
\end{aligned}
$$

where $\{\lambda_j\}$ are F Lagrange multipliers. In Eq. (23), we assume that the frame data are cyclic and then 0th frame data exactly coincide with the Fth frame data, that is, $x_0(n) = x_F(n)$ and $\mathbf{k}_0 = \mathbf{k}_F$. The second term in the right-hand side of Eq. (23) shows the constraint for the spectrum transition between the successive frames. The denominator $|\mathbf{x}_j|^2$ of the first term in the right-hand side normalizes the signal power of jth frame data.

In this logarithmic likelihood function ℓ, if $\{\lambda_j\}$ are set to be large, the second term of Eq. (23) is dominant and then the maximization of ℓ corresponds to the solution so as to be $|\mathbf{k}_{j+1} - \mathbf{k}_j|^2 = 0$, for $j = 0, 1, \ldots, F-1$. However, this procedure does not at all take into consideration the spectrum estimation which is achieved by the minimization of $\alpha_{M,j}$ in Eq. (22).

On the other hand, if the values of $\{\lambda_j\}$ are set to be very small, the second term of Eq. (23) is negligible and then only its first term is dominant. Thus, it is important to select appropriate values of $\{\lambda_j\}$. In this paper, the values are set uniformly for the subjects in *in vivo* experiments so that the resultant spectrum transition patterns become reasonable from the cardiological side and the differences between the healthy subjects and the patient are clear.

Let us determine the PARCORR coefficients $\{\mathbf{k}_j\}$ which maximize the logarithmic likelihood function ℓ as follows. Let us assume that F Lagrange multipliers $\{\lambda_j\}$ are the same value of λ. By taking the partial derivative of ℓ with respect to $\{\mathbf{k}_j\}$ and setting the results to be zero, the following simultaneous equations are obtained.

$$
\begin{aligned}
&-\frac{1}{2} \frac{\partial \ell}{\partial \mathbf{k}_j} \\
&\quad = \frac{1}{|\mathbf{x}_j|^2} \left(\mathbf{\Delta}_j \mathbf{k}_j + \mathbf{B}_j^T \mathbf{c}_j \right) + \lambda \left(2\mathbf{k}_j - \mathbf{k}_{j-1} - \mathbf{k}_{j+1} \right) \\
&\quad = 0. \qquad (24)
\end{aligned}
$$

By solving Eq. (24), the PARCORR coefficients $\{\mathbf{k}_j\}$ of all frame data are estimated under the constraint for the spectrum transition between the frame data.

From Eq. (24),

$$\left(\frac{\mathbf{\Delta}_j}{|\mathbf{x}_j|^2} + 2\lambda \mathbf{I} \right) \mathbf{k}_j - \lambda \mathbf{k}_{j-1} - \lambda \mathbf{k}_{j+1} = -\frac{\mathbf{B}_j^T \mathbf{c}_j}{|\mathbf{x}_j|^2}, \qquad (25)$$

where $\mathbf{I}$ is the $M \times M$ identity matrix. Let us denote $(\mathbf{\Delta}_j / |\mathbf{x}_j|^2 + 2\lambda \mathbf{I})$ by an $M \times M$ diagonal matrix $\mathbf{D}_j$ and let us define an $FM \times FM$ matrix $\mathbf{G}$ and FM-dimension vectors $\mathbf{g}$ and $\mathbf{k}$ as follows:

$$\mathbf{G} = \begin{bmatrix} \mathbf{D}_0 & -\lambda\mathbf{I} & 0 & \cdots & 0 & -\lambda\mathbf{I} \\ -\lambda\mathbf{I} & \mathbf{D}_1 & -\lambda\mathbf{I} & 0 & \cdots & 0 \\ 0 & -\lambda\mathbf{I} & \mathbf{D}_2 & \ddots & \ddots & \vdots \\ \vdots & 0 & \ddots & \ddots & \ddots & 0 \\ 0 & \vdots & \ddots & \ddots & \ddots & -\lambda\mathbf{I} \\ -\lambda\mathbf{I} & 0 & \dots & 0 & -\lambda\mathbf{I} & \mathbf{D}_{F-1} \end{bmatrix}, \tag{26}$$

$$\mathbf{g} = \left[\left(\frac{\mathbf{B}_0^T \mathbf{c}_0}{|\mathbf{x}_j|^2} \right)^T, \cdots, \left(\frac{\mathbf{B}_{F-1}^T \mathbf{c}_{F-1}}{|\mathbf{x}_{F-1}|^2} \right)^T \right]^T, \tag{27}$$

$$\mathbf{k} = \left[\mathbf{k}_0^T, \mathbf{k}_1^T, \dots, \mathbf{k}_{F-1}^T \right]^T. \tag{28}$$

Using these matrix and vectors, optimum estimation of the spectrum transition of a nonstationary signal under the constraint for the spectrum transition between frame data is simultaneously achieved by solving the following linear simultaneous equations:

$$\mathbf{G}\mathbf{k} = -\mathbf{g}, \tag{29}$$

where the term $-\lambda\mathbf{I}$ in the top right and bottom left of the matrix $\mathbf{G}$ is introduced by assuming $x_0(n) = x_F(n)$. Therefore, the PARCORR coefficients of the multi-frame data are simultaneously estimated by

$$\widehat{\mathbf{k}} = -\mathbf{G}^{-1}\mathbf{g}, \tag{30}$$

where $\mathbf{G}^{-1}$ is the inverse matrix of $\mathbf{G}$. Using the estimates $\widehat{\mathbf{k}} = \left[\widehat{\mathbf{k}}_0^T, \widehat{\mathbf{k}}_1^T, \dots, \widehat{\mathbf{k}}_{F-1}^T \right]^T$, estimates of the vectors $\mathbf{a}_j$ of linear predictive coefficients in the jth frame data are obtained by

$$\widehat{\mathbf{a}}_j = \mathbf{B}_j \widehat{\mathbf{k}}_j. \quad (j = 0, 1, \dots, F-1) \tag{31}$$

4. *In vivo* Experiments for Estimation of the Spectrum Transition of the Vibrations on the Heart Wall

We applied this method to the analysis of the velocity signals measured in our laboratory using a noninvasive measurement method [12] on the interventricular septum (IVS) in the heart wall of two healthy male subjects and a patient with acute lymphoblastic leukemia and serious doxorubicin-cardiomyopathy, who had been treated with an anti-cancer drug (antracenadiones).

Figure 1 shows a standard brightness (B)-mode short-axis image of the cross-sectional area around the detected points preset in the IVS of a presumedly healthy 26-year-old male volunteer. The ultrasonic beam passing through the two points of R and L is almost perpendicular to the IVS during the measurements.

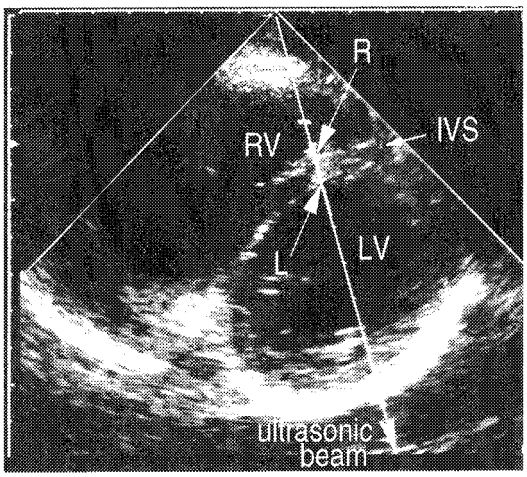

Fig. 1 A standard B-mode short-axis image showing the cross-sectional area around the detected points preset in the interventricular septum (IVS) in an *in vivo* experiment for the detection of their instantaneous positions and the velocity signals of a presumedly healthy 26-year-old male volunteer. Points (R) and (L) are on the RV surface and the LV surface of the IVS, respectively.

4.1 Waveforms for Spectrum Analysis

Figures 2 (1-a) and (1-b) show the electrocardiogram (ECG) and the heart sound (PCG), respectively, of the 26-year-old healthy male subject in Fig. 1. Figure 2 (1-c) shows the velocity signals $\{v_i(t)\}$ $(i = 0, 1, \dots, 13)$ measured for the 14 points preset from the right ventricular (RV) surface (the point R in Fig. 1) to the left ventricular (LV) surface (the point L in Fig. 1) of the IVS. The 14 velocity signals are overlaid.

From the signals in Fig. 2 (1-c), the time-differential waveforms $\{v_i'(t)\}$ of the velocity signals $\{v_i(t)\}$, which are the acceleration signals, are obtained to emphasize higher frequency components as shown in Fig. 2 (1-d). The original sampling frequency is 4.5 kHz. The signals $\{v_i'(t)\}$ are re-sampled at a frequency of 200 Hz so that they are analyzed in the frequency range up to 100 Hz. Figure 2 (2) shows the waveforms for the 32-year-old male patient.

One heartbeat signal $v_i'(t)$ on the LV side of the IVS in Figs. 2 (1-d) and (2-d) is divided into multiple frame signals $\{v_i'(n; j)\}$, $(j = 0, 1, \dots, F-1;\ n = 0, 1, \dots, N-1)$, each of which is $N = 20$ points (100 ms) in length, which roughly corresponds to the duration of the first heart sound. Adjacent frame signals overlap each other by a three-quarter length (75 ms). For the signals in Figs. 2 (1-d) and (2-d), the numbers (F) of the preset frames are 47 and 33, respectively, which are determined by the length of one cardiac cycle.

4.2 Estimates of the Spectrum Transition

By applying the proposed method ($M = 6$) to the accel-

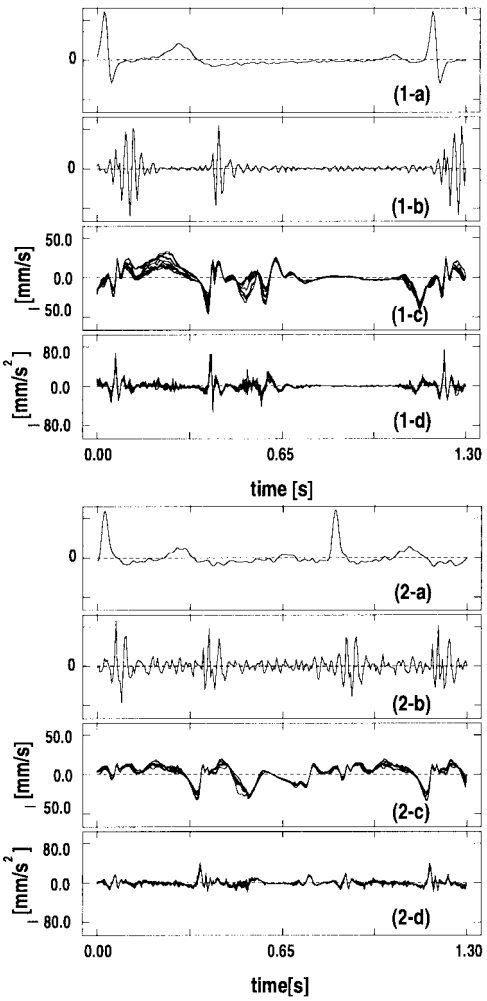

Fig. 2 (a) ECG, (b) PCG, (c) velocity signals $\{v_i(t)\}$, (d) acceleration signals $\{v_i^{'}(t)\}$ of (c). (1) for the healthy male subject in Fig. 1 and (2) for a 32-year-old male patient.

eration signals $v_{13}^{'}(t)$ on the LV surface in Fig. 2 (1-d), the resultant spectrum transition patterns are shown in Fig. 3 (a). The center frequency of each estimated pole is indicated by a circle. In these experiments, the value of λ of Eq. (23) is set as 0.316.

Figure 3 (b) shows the results obtained by applying the same procedure to the acceleration signal of a 22-year-old healthy male subject.

On the other hand, Figs. 3 (c) and (d) show the spectrum transition patterns of the acceleration signal on the LV surface of the IVS for a 32-year-old male patient. The data analyzed in Figs. 3 (c) and (d) (also in Fig. 2 (2)) were measured five months and two months before his death, respectively.

For the same acceleration signals in Figs. 3 (a) and (c), the instantaneous spectrum patterns are estimated without using the transition constraint, that is, $\lambda = 0$. The results are shown in Figs. 4 (a) and (c), respectively. These results correspond to those obtained by independently applying the standard AR estimation method to each frame signal. By comparing the estimates in Figs. 3 (a) and (c) with those in Figs. 4 (a) and (c), the introduction of the constraint in Eq. (23) is found to be effective.

4.3 Discussion

1. For the data in Figs. 3 (c) and (d) of the patient, it is found that the duration of diastole becomes shorter, while that of systole is still almost the same as those of the normal subjects in Figs. 3 (a) and (b).
2. Since clear components of the heart sound have not been recognized for healthy subjects in the diastole from the end of the second heart sound (II) to the beginning of the first heart sound (I), analysis of the heart sound in diastole has not been reported in the literature. As shown by the ovals in Figs. 3 (a)–(d), however, there are the remarkable spectrum peaks between 10 Hz and 20 Hz for both the normal subjects and the patient. Moreover, the dominant frequencies gradually become lower from the beginning to the end of diastole, which corresponds to the dilation of the LV.
3. By comparing the results in Figs. 3 (a) and (b) with those in Figs. 3 (c) and (d), the power of the normal subjects is seen to be large in the frequency range up to 100 Hz around the radiation timing of the second heart sound (II), which corresponds to the period from the end-systole to the beginning of diastole.

   For the patient, however, the power decreased, especially in the higher frequency band. These phenomena correspond to the myocardial defect which occurred due to the dose of the anti-cancer drug [13].
4. In systole, since there is a large difference among individual subjects, remarkable characteristics have not yet been recognized. For the radiation timing of the first heart sound (I), however, the power of the patient in Figs. 3 (c) and (d) decreases, especially at higher frequencies.

5. *In vivo* Experiments for Estimation of the Spatial-Transition of the Spectra of the Vibrations on the Heart Wall

Figures 5 (1) and (2) show the acceleration signals at the 14 points preset at even intervals of 0.75 mm from the RV side to the LV side of the IVS for the normal subject in Fig. 2 (1) and the patient in Fig. 2 (2), respectively. The one cardiac signal is divided into several periods, each of which is shown in these figures.

Figures 6 (1) and (2) show the spectrum transition

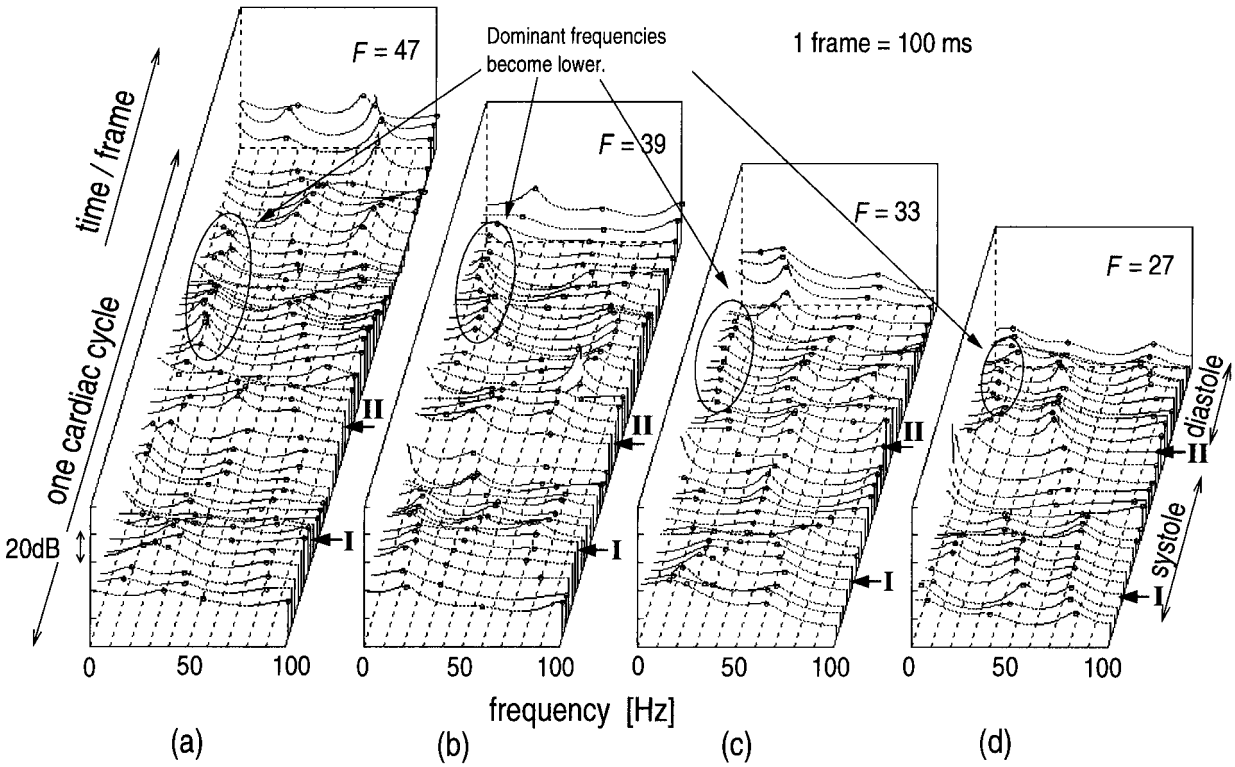

Fig. 3 Spectrum transition pattern of the acceleration signal on the heart wall for one cardiac cycle (circle: the center frequency of each estimated pole). (a) the 26-year-old healthy male subject, (b) a 22-year-old healthy male subject, (c) a 32-year-old male patient (five months before death), (d) the same 32-year-old male patient (two months before death). "I" and "II" show the radiated timing of the first and the second heart sounds.

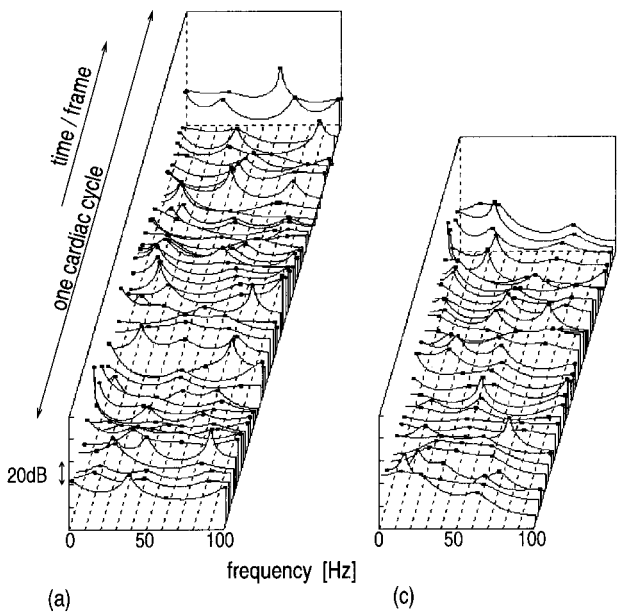

Fig. 4 Spectrum transition pattern of the acceleration signal estimated without using the transition constraint, that is, $\lambda = 0$. (a) the 26-year-old healthy male subject in Fig. 3 (a), (c) the 32-year-old male patient (five months before death) in Fig. 3 (c).

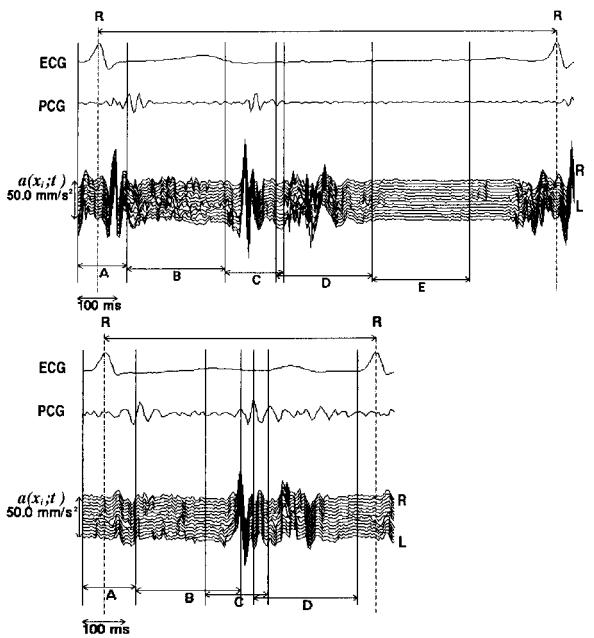

Fig. 5 The acceleration signals from the RV to the LV and their analyzed periods from A to E or from A to D. Upper: for the normal subject in Fig. 2 (1). Lower: for the patient in Fig. 2 (2).

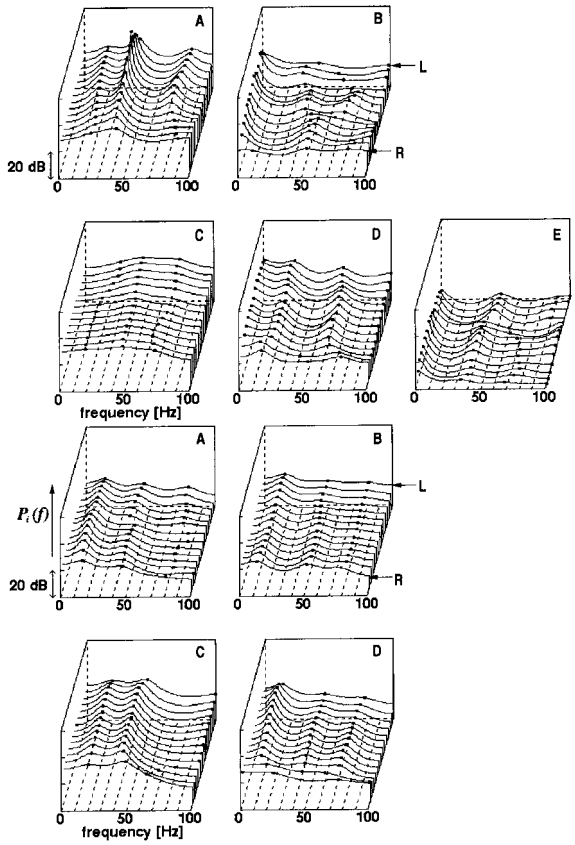

Fig. 6 The spatial transition pattern of the estimated spectra from the RV to the LV for each period from A to E or from A to D indicated in Fig. 5 (circles: the center frequency of each estimated pole). Upper 5 figures: for the normal subject. Lower 4 figures: for the patient.

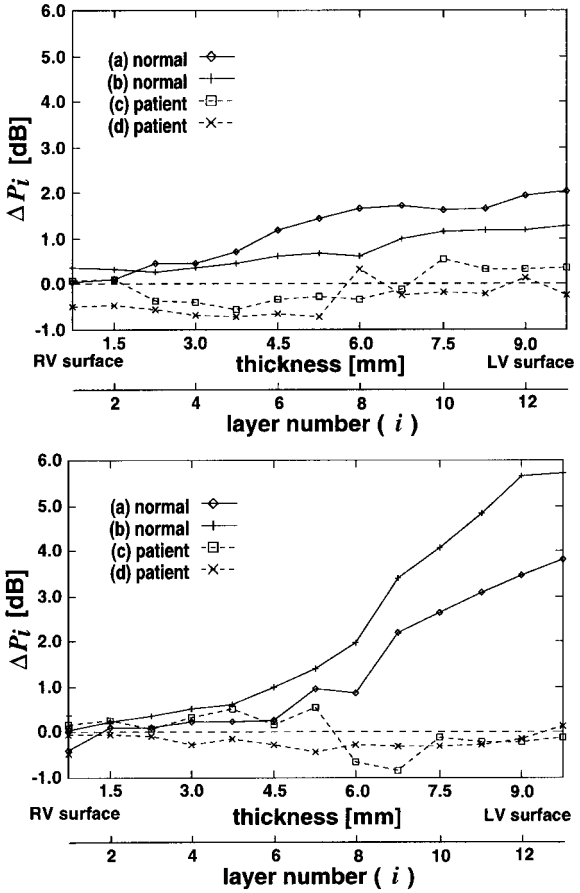

Fig. 7 The average value ΔP_i of the difference of the power spectrum $P_i(f)$ of the ith layer from the power spectrum $P_R(f)$ of the RV side in the frequency range from d.c. to 100 Hz for four subjects in Fig. 3. upper: for the period A around the R-wave. lower: for the period C around the second heart sound (II).

patterns obtained by applying the proposed method ($M = 6$) to the sectional signals in each of the periods from A to E of Fig. 5 (1) and from A to D of 5 (2), respectively.

For the 3 subjects, the average value ΔP_i of the difference of the power spectrum $P_i(f)$ of the ith layer from the power spectrum $P_R(f)$ of the RV side in the frequency range from d.c. to 100 Hz is evaluated for the periods of A and C as follows:

$$\Delta P_i = \frac{1}{101}\sum_{f=0}^{100}(P_i(f) - P_R(f)). \tag{32}$$

The results are shown in Fig. 7.

From Figs. 6 and 7, for the normal subject, there are large changes in power among the signals from the RV side to the LV side, especially in period A (at the beginning of the systole), period C (from the end-systole to the beginning of the diastole), and period D (diastole). That is, the power on the LV side is larger than the power on the RV side. This increase in power shows that there is a large change in thickness in the IVS during each period for the normal subject.

For the patient, however, such remarkable phenomena were not observed in any period, which corresponds to the decrease in thickness of the IVS in the serious patient.

If the myocardium is a passive component, these values of the change in thickness directly correspond to the strain in the heart wall and its elasticity may be evaluated using the blood pressure. However, since the myocardium itself is not a passive component, but rather an active component, it will be difficult to estimate the elasticity of the myocardium from the obtained change in thickness in this paper.

6. Conclusions

We have presented a new method for estimation of the spectrum transition of a nonstationary signal in low SNR cases using a linear algorithm. Applying the proposed method to heart wall vibrations, we found clear spectrum transition patterns.

The small velocity signals accurately measured by

our method contain sufficient information to diagnose the acoustic characteristics of the heart muscle during one cardiac cycle. Thus, the measurement of the heart wall vibrations and their analysis as proposed in this paper are expected to lead to the development of a new scientific field of noninvasive diagnosis of heart dysfunction.

In this paper, the order M of the AR model was fixed to be 6 based on our previous analysis of the fourth heart sound in [10], and $\lambda = 0.316$ was employed as the value of the Lagrange multipliers based on *in vivo* experiments using two healthy subjects and one patient. It is, however, necessary to develop a method for deciding the order M of the AR model and values of the Lagrange multipliers. These problems are under investigation.

Acknowledgments

The authors would like to thank Prof. Noriyoshi Chubachi of Tohoku Gakuin University, Prof. Motonao Tanaka of Tohoku Kousei-Nenkin Hospital, Dr. Yoshiko Saito of Tohoku University School of Medicine, Dr. Yoshiro Uzuka of the Sendai Center for Hematologic Disorders, and Miss Michie Sato for their helpful comments and their support in the *in vivo* experiments.

References

[1] T.S. Rao, "The fitting of non-stationary time-series models with time-dependent parameters," J. of the Royal Statist. Soc. Series B, vol.32, no.2, pp.312–322, 1970.
[2] L.A. Liporace, "Linear estimation of non-stationary signals," J. Acoust. Soc. Amer., vol.58, no.6, pp.1288–1295, 1975.
[3] K.C. Sharman and B. Friedlander, "Time-varying autoregressive modeling of a class of nonstationary signals," Proc. IEEE ICASSP, pp.22.2.1–22.2.4, 1984.
[4] F. Kozin, "Estimation and modeling of nonstationary time-series," Proc. Symp. Appl. Comput. Meth. Eng., vol.1, Los Angeles, CA, pp.603–612, 1977.
[5] G. Alehgrin, M. Barlaud, and J. Menez, "Unbiased parameter estimation of nonstationary signals and noise," IEEE Trans. ASSP, vol.ASSP-34, no.5, pp.1319–1322, 1986.
[6] M. Hall, A.V. Oppenheim, and A. Willsky, "Time-varying parametric modeling of speech," Proc. IEEE Decision and Control Conf., New Orleans, LA, pp.1085–1091, 1977.
[7] Y. Grenier, "Time-dependent ARMA modeling of nonstationary signals," IEEE Trans. ASSP, vol.ASSP-31, no.4, pp.899–911, 1983.
[8] M.J. Flaherty, "Application of polynomial splines to a time-varying autoregressive model of speech," Proc. IEEE ICASSP, pp.2220–2223, 1988.
[9] E. Karlsson and M.H. Hayes, "ARMA modeling of time-varying systems with lattice filters," Proc. IEEE ICASSP, pp.2335–2338, 1986.
[10] H. Kanai, N. Chubachi, K. Kido, Y. Koiwa, T. Takagi, J. Kikuchi, and T. Takishima, "A new approach to time-dependent AR modeling of signals and its application to analysis of the fourth heart sound," IEEE Trans. SP, vol.40, no.5, pp.1198–1205, 1992.
[11] H. Kanai, K. Hirose, H. Sato, and N. Chubachi, "A new method for measuring small local vibrations in the heart using ultrasound," IEEE Trans. BE, vol.40, no.12, pp.1233–1242, 1993.
[12] H. Kanai, M. Sato, Y. Koiwa, and N. Chubachi, "Transcutaneous measurement and spectrum analysis of heart wall vibrations," IEEE Trans. UFFC, vol.43, no.5, pp.791–810, 1996.
[13] H. Kanai, H. Hasegawa, N. Chubachi, Y. Koiwa, and M. Tanaka, "Noninvasive evaluation of local myocardial thickening and its color-coded imaging," IEEE Trans. UFFC, vol.44, no.4, pp.752–768, 1997.
[14] J.D. Markel and A.H. Gray, Jr., "Linear prediction of speech," Springer-Verlag, 1978.
[15] S.M. Kay, "Modern spectral estimation," Prentice Hall, Chapter 6, 1987.

Hiroshi Kanai was born in Matsumoto, Japan, on November 29, 1958. He received the B.E. degree from Tohoku University, Sendai, Japan in 1981, and the M.E. and the Dr.Eng. degrees, also from Tohoku University, in 1983 and 1986, both in Electrical Engineering. From 1986 to 1988, he was with the Education Center for Information Processing, Tohoku University, as a Research Associate. From 1990 to 1992, he was a Lecturer in the Department of Electrical Engineering, Faculty of Engineering, Tohoku University. Since 1992, he has been an Associate Professor in the Department of Electrical Engineering, Faculty of Engineering, Tohoku University. His present interest is in ultrasonic measurements and digital signal processing for diagnosis of the heart diseases and atherosclerosis. Dr. Kanai is member of the Acoustical Society of Japan, the Japan Society of Ultrasonics in Medicine, the Japan Society of Medical Electronics and Biological Engineering, the Institute of Electrical Engineers of Japan, the Japanese Circulation Society, the Japanese College of Cardiology, and the IEEE.

Yoshiro Koiwa was born in Sendai, Japan, in 1944. He graduated from Tohoku University, Sendai, Japan, in 1969. He received the M.D. degree from Tohoku University in 1977. He is presently Associate Professor of Internal Medicine of Tohoku University. His main research interest is cardiovascular disease, especially cardiac function and heart failure. Dr. Koiwa is member of American Federation for Clinical Research, the Japanese Circulation Society, and the Japan Society of Medical Electronics and Biological Engineering.